Bondi Flow from a Slowly Rotating Hot Atmosphere

Monthly Notices
of the
ROYAL ASTRONOMICAL SOCIETY

Mon. Not. R. Astron. Soc. **415,** 3721–3730 (2011) doi:10.1111/j.1365-2966.2011.18987.x

Bondi flow from a slowly rotating hot atmosphere

Ramesh Narayan[1]★ and Andrew C. Fabian[2]★

[1]*Harvard-Smithsonian Center for Astrophysics, 60 Garden Street, Cambridge, MA 02138, USA*
[2]*Institute of Astronomy, Madingley Road, Cambridge CB3 0HA*

Accepted 2011 April 29. Received 2011 April 29; in original form 2011 March 10

ABSTRACT

A supermassive black hole in the nucleus of an elliptical galaxy at the centre of a cool-core group or cluster of galaxies is immersed in hot gas. Bondi accretion should occur at a rate determined by the properties of the gas at the Bondi radius and the mass of the black hole. X-ray observations of massive nearby elliptical galaxies, including M87 in the Virgo cluster, indicate a Bondi accretion rate $\dot{M}_{\rm B}$ which roughly matches the total kinetic power of the jets, suggesting that there is a tight coupling between the jet power and the mass accretion rate. While the Bondi model considers non-rotating gas, it is likely that the external gas has some angular momentum, which previous studies have shown could decrease the accretion rate drastically. We investigate here the possibility that viscosity acts at all radii to transport angular momentum outwards so that the accretion inflow proceeds rapidly and steadily. The situation corresponds to a giant advection-dominated accretion flow (ADAF) which extends from beyond the Bondi radius down to the black hole. We find solutions of the ADAF equations in which the gas accretes at just a factor of a few less than $\dot{M}_{\rm B}$. These solutions assume that the atmosphere beyond the Bondi radius rotates with a sub-Keplerian velocity and that the viscosity parameter is large, $\alpha \geq 0.1$, both of which are reasonable for the problem at hand. The infall time of the ADAF solutions is no more than a few times the free-fall time. Thus, the accretion rate at the black hole is closely coupled to the surrounding gas, enabling tight feedback to occur. We show that jet powers of a few per cent of $\dot{M}_{\rm B}c^2$ are expected if either a fraction of the accretion power is channelled into the jet or the black hole spin energy is tapped by a strong magnetic field pressed against the black hole by the pressure of the accretion flow. We discuss the Bernoulli parameter of the flow, the role of convection and the possibility that these as well as magnetohydrodynamic effects may invalidate the model. If the latter comes to pass, it would imply that the rough agreement between observed jet powers and the Bondi accretion rate is a coincidence and jet power is determined by factors other than the mass accretion rate.

Key words: accretion, accretion discs – black hole physics – galaxies: clusters: intracluster medium – galaxies: jets – galaxies: nuclei – X-rays: galaxies.

1 INTRODUCTION

The nuclei of massive elliptical galaxies at the centres of cool-core groups and clusters of galaxies have powerful relativistic jets which inject energy into the surrounding hot gas. This prevents the intracluster gas from radiatively cooling and collapsing on to the galaxy, thus stifling its growth (McNamara & Nulsen 2007, and references therein). Such feedback is now a common ingredient in our understanding of the evolution of massive galaxies (Croton et al. 2006; Hopkins et al. 2006).

The mode of fuelling of the massive black hole at the galaxy nucleus, which energizes the jets, is unclear. Bondi (1952) accretion is often invoked since the black hole is sitting in the densest part of the hot cluster (or group) atmosphere. Observations of the gas around the Bondi radius in M87 indicate that Bondi accretion may indeed provide a suitable mass supply rate (di Matteo et al. 2003). Others argue that it cannot provide enough fuel to power more powerful, distant objects (Rafferty et al. 2006), and that cold gas clouds may instead be required (Pizzolato & Soker 2005). Regardless, the Bondi model considers gas with vanishing angular momentum, whereas in a realistic situation the incoming gas is likely to have non-negligible rotation. Hence, it is not clear that the Bondi accretion rate $\dot{M}_{\rm B}$ is at all relevant.

★E-mail: rnarayan@cfa.harvard.edu (RN); acf@ast.cam.ac.uk (ACF)

Most nuclei in the centres of cool-core clusters show no sign of a dense, radiatively efficient accretion disc. Some of the most powerful ones do not even show any detectable X-ray point source (Hlavecek-Larrondo & Fabian 2011), which is difficult to explain in cold-mode accretion. In the case of M87, there is clear evidence that both the accretion flow and the jets themselves are radiatively inefficient (di Matteo et al. 2003). This indicates that the flow must be advection-dominated, i.e. the gravitational energy released in the flow must be carried into the centre rather than radiated locally [see Narayan, Mahadevan & Quataert 1998; Kato, Fukue & Mineshige 2008; Narayan & McClintock 2008 for reviews of advection-dominated accretion flows (ADAFs)]. A fraction of the energy must then be efficiently transferred to the jets once the accreting gas reaches the centre.

The above conclusion is supported by a study of eight other massive nearby elliptical galaxies where the gas properties close to the Bondi radius can be observed or reasonably extrapolated (Allen et al. 2006). In all these cases, the Bondi mass accretion rate $\dot{M}_{\rm B}$ determined at the Bondi radius $r_{\rm B}$ correlates well with the power of the jets $P_{\rm j}$, where the latter is measured from the bubbles inflated by the jets in the surrounding gas. Writing the jet power as $P_{\rm j} = \eta_{\rm j}\dot{M}_{\rm B}c^2$, the jet production efficiency factor $\eta_{\rm j}$ is found to be about 2 per cent. This is a rather large efficiency and underscores the need for mass at approximately the Bondi accretion rate reaching the gravitational radius of the black hole $r_{\rm g}$. There is little room for any inefficiency in the transport of mass to the centre, e.g., through mass loss in outflows along the way.

We are concerned here whether an ADAF can be established in galactic nuclei and whether the mass accretion rate is comparable to the Bondi rate. The range of jet power in the systems discussed above is between 10^{43} and $10^{45}\,{\rm erg\,s^{-1}}$, so the Eddington ratio (power emitted to the Eddington limit) is 10^{-4}–10^{-2} for a black hole of mass $10^9\,{\rm M}_\odot$, and 10 times less for $10^{10}\,{\rm M}_\odot$. This is very much in the regime where an ADAF is expected (Narayan & Yi 1995b; Narayan & McClintock 2008). Moreover, as noted by Narayan & Yi (1994, 1995a) and Fabian & Rees (1995), and confirmed in more recent investigations (Narayan & McClintock 2008), the large thermal pressure of an ADAF may be especially good for the production and collimation of jets. Thus, it is natural to consider an ADAF-like accretion model for systems with powerful jets.

ADAFs have been well studied since the work of Narayan & Yi (1994, 1995a,b) and Abramowicz et al. (1995). However, in much of the previous work, the outer edge of the solution was generally taken to be either of a self-similar form (e.g. Chen, Abramowicz & Lasota 1997; Popham & Gammie 1998) or a geometrically thin disc that evaporates to form the ADAF (e.g. Narayan, Kato & Honma 1997; Manmoto et al. 2000). Neither of these boundary conditions is relevant for understanding accretion from an external medium. Since an ADAF is essentially space filling, we expect the accretion flow to match smoothly on to the external medium without any shocks or other kinds of discontinuities. We investigate in this paper exactly how this matching occurs when we have a slowly rotating external medium (equation 23 gives a quantitative measure of what we mean by slow rotation).

Previous studies of Bondi-like accretion with angular momentum have generally considered inviscid flows. Proga & Begelman (2003) carried out two-dimensional axisymmetric simulations and showed that an equatorial torus forms because of the angular momentum barrier and that this torus constrains the amount of polar accretion. Krumholz, McKee & Klein (2005) extended their work and developed approximate formulae for the mass accretion rate as a function of the vorticity of the external gas, and Cuadra et al. (2006) carried out detailed simulations of inviscid accretion on to Sagittarius A* at the Galactic Centre. Recently, Inogamov & Sunyaev (2010) proposed an accretion model for M87. As in the other studies cited here, the centrifugal barrier causes the inviscid accreting gas to form a torus well inside $r_{\rm B}$. Inogamov & Sunyaev assume that viscosity then turns on at smaller radii and suggest that the torus will thus feed a standard thin accretion disc on the inside, which might evaporate into an ADAF at yet smaller radii. The presence of the thin disc segment in their model causes the total inflow time of the gas from the Bondi radius $r_{\rm B}$ to the black hole gravitational radius $r_{\rm g}$ to be far longer than for a Bondi flow or (as we shall see) an ADAF. Self-adjustment of the feedback, in which the jet power responds to conditions (e.g. cooling time) beyond $r_{\rm B}$, then becomes very difficult, with large hysteresis expected.

In contrast to the above studies, we are interested in viscous accretion. The closest paper to our work is Park (2009). For technical reasons, that work focused on extremely hot external media ($T_{\rm ext} > 10^9$ K) for which the Bondi radius is much closer to the black hole than in real systems. We consider more realistic external conditions ($T_{\rm ext} \sim 10^{6-7}$ K). We also study in more detail the transition from a Bondi flow to an ADAF as the external rotation is varied.

As in Park (2009), we require the flow to be continuous from the event horizon of the black hole to beyond the Bondi radius $r_{\rm B}$. Such a model ensures that the accretion power is as well coupled with the conditions in the outer gas as possible, thereby allowing for the most efficient feedback. We, moreover, require that outflows, and significant radial exchanges of energy within the ADAF, are suppressed. We postulate that relativistic jets are created and mechanically powered very efficiently (but very radiatively inefficiently) by the accreting gas close to the black hole, but how this occurs is beyond the scope of the present work. We limit ourselves to a more basic question: can an idealized ADAF transfer a high enough mass accretion rate from beyond $r_{\rm B}$ down to $r_{\rm g}$?

2 SPHERICAL ADAF MODEL

2.1 Viscous accretion flow: conservation laws

Since we are primarily interested in slowly rotating, steady, viscous accretion flows, we assume that the density and pressure of the gas are distributed spherically at each radius. We also assume that all quantities are independent of time (steady-state assumption). We thus focus only on radial variations. Under these assumptions, the mass accretion rate $\dot{M}$ at radius r is given by

$$\dot{M} = -4\pi r^2 \rho v = \text{constant}, \tag{1}$$

where $\rho(r)$ is the density and $v(r)$ is the radial velocity; the latter is taken to be negative when gas flows inwards. When considering accretion flows in which rotational support is important, e.g. geometrically thin discs, or ADAFs with more rotation than we consider here, the factor $4\pi r^2$ in the above relation is replaced by $(2\pi r)(2H)$, where $H(r)$ is the 'vertical' scaleheight of the gas at radius r. In the simpler approximation considered here, we effectively set $H = r$, which could be interpreted as a geometrically very thick disc. Except for this difference, the equations we consider are identical to those described in Narayan et al. (1997).

To mock up relativistic gravity in our Newtonian model, we assume a gravitational potential (Paczyński & Wiita 1980)

$$\phi(r) = -\frac{GM}{(r - r_{\rm g})}, \qquad r_{\rm g} = \frac{2GM}{c^2}, \tag{2}$$

where M is the mass of the central black hole. Correspondingly, the Keplerian angular frequency $\Omega_{\rm K}$ is given by

$$\Omega_{\rm K}^2 = \frac{GM}{(r-r_{\rm g})^2 r}. \tag{3}$$

Making the replacement $p = \rho c_{\rm s}^2$, where $c_{\rm s}$ is the (isothermal) sound speed, we write the steady-state radial momentum equation as

$$v\,\frac{{\rm d}v}{{\rm d}r} = -\left(\Omega_{\rm K}^2 - \Omega^2\right) r - \frac{1}{\rho}\,\frac{\rm d}{{\rm d}r}\left(\rho c_{\rm s}^2\right), \tag{4}$$

where Ω is the angular velocity of the gas on the equatorial plane. Our spherical model is most accurate when the centrifugal acceleration on the gas is much weaker than the gravitational acceleration; this corresponds to the condition $\Omega^2 \ll \Omega_{\rm K}^2$.

We model viscosity via the standard α-prescription (Shakura & Sunyaev 1973) in which the kinematic coefficient of viscosity ν is written as

$$\nu = \alpha c_{\rm s} H = \alpha c_{\rm s} r, \tag{5}$$

with α taken to be a constant. However, we do not set the shear stress equal to αp, but use a more physical prescription in which the stress is proportional to the angular velocity gradient:

$$\text{shear stress} \equiv \sigma_{r\phi} = \nu\rho r\,{\rm d}\Omega/{\rm d}r. \tag{6}$$

The angular momentum equation then takes the form (Narayan et al. 1997)

$$v\frac{\rm d}{{\rm d}r}(\Omega r^2) = \frac{1}{\rho r^2}\frac{\rm d}{{\rm d}r}\left(\alpha\rho c_{\rm s} r^5 \frac{{\rm d}\Omega}{{\rm d}r}\right), \tag{7}$$

which on integration gives

$$\frac{{\rm d}\Omega}{{\rm d}r} = \frac{v(\Omega r^2 - j)}{\alpha r^3 c_{\rm s}}. \tag{8}$$

The quantity j is an integration constant with dimensions of specific angular momentum.

Finally, energy conservation gives

$$\frac{\rho v}{(\gamma-1)}\frac{{\rm d}c_{\rm s}^2}{{\rm d}r} - c_{\rm s}^2 v\frac{{\rm d}\rho}{{\rm d}r} = \alpha\rho c_{\rm s} r^3\left(\frac{{\rm d}\Omega}{{\rm d}r}\right)^2, \tag{9}$$

where γ is the adiabatic index of the gas, which is set to 5/3 for all the numerical models presented here. The left-hand side of equation (9) represents the Lagrangian time derivative of the entropy of the gas. This term is usually referred to as the energy advection term. The term on the right-hand side of the equation describes the heating rate due to viscous dissipation. In the spirit of a radiatively inefficient flow (ADAF), we ignore radiative cooling altogether. Thus, we set advection equal to heating to obtain equation (9).

We should note the following inconsistency in the above equations.[1] While we have included the effect of viscosity through the shear stress in the angular momentum equation (7), we have neglected corresponding terms in the radial momentum equation (4). Under the assumptions of our model (pure radial flow, no gradients in the transverse direction, etc.), the rr component of the stress takes the form (Landau & Lifshitz 1959)

$$\sigma_{rr} = -\rho c_{\rm s}^2 + \frac{4}{3}\eta\rho r\frac{{\rm d}(v/r)}{{\rm d}r} + \xi\rho\frac{1}{r^2}\frac{{\rm d}(r^2 v)}{{\rm d}r}, \tag{10}$$

where ξ is the kinematic bulk viscosity. The last term in equation (4) should thus be written as $(1/\rho)\,{\rm d}(\sigma_{rr})/{\rm d}r$ with the above form of σ_{rr}, not just as $-(1/\rho)\,{\rm d}(\rho c_{\rm s}^2)/{\rm d}r$.

[1] We thank the referee for pointing this out to us.

Traditionally, in accretion disc models, the viscous terms in σ_{rr} are neglected on the grounds that v is much smaller than $c_{\rm s}$ and so these terms are small compared to the pressure. This is no longer obvious for the slowly rotating solutions presented here, for which v is fairly large. Nevertheless, we make this assumption for easy comparison with previous work. A major goal of the present work is to study the transition from the rapidly rotating ADAF regime to the non-rotating Bondi regime. The viscous terms in σ_{rr} survive even for pure radial flow and ought to be included in a self-consistent model of spherical inflow. Since these terms are neglected in the Bondi model, in the same spirit we neglect them in our model as well. We leave for the future an investigation of the effect of these terms on both the Bondi solution and our slowly rotating solution.

2.2 The inner supersonic region

The equations in Subsection 2.1 correspond to a viscous rotating accretion flow. Once the accreting gas passes inside the sonic radius $r_{\rm s}$ and becomes supersonic, we expect viscosity to be much reduced and perhaps even to vanish (Narayan 1992; Kato & Inagaki 1994; Kley & Papaloizou 1997). For this region of the flow, we simplify the equations by setting $\alpha = 0$, thus dropping all terms related to viscosity. From the angular momentum equation (7), we see that the specific angular momentum is then a constant:

$$r < r_{\rm s}: \quad \ell_{\rm in} \equiv \Omega r^2 = \text{constant}. \tag{11}$$

Similarly, from the energy equation (9), we see that the entropy of the gas is constant:

$$r < r_{\rm s}: \quad s_{\rm in} \equiv \frac{c_{\rm s}^2}{\rho^{(\gamma-1)}} = \text{constant}. \tag{12}$$

Finally, by combining the various conservation laws, we can show that the Bernoulli parameter $\mathcal{B}$ of the gas is also constant. This gives the condition

$$\begin{aligned} r < r_{\rm s}: \quad \mathcal{B} \equiv{}& \frac{v^2}{2} + \frac{\ell_{\rm in}^2}{2r^2} - \frac{GM}{(r-r_{\rm g})} \\ &+ \frac{\gamma\, s_{\rm in}}{(\gamma-1)\, r^{2(\gamma-1)}\, |v|^{(\gamma-1)}}\left(\frac{\dot M}{4\pi}\right)^{(\gamma-1)} \\ ={}& \text{constant}. \end{aligned} \tag{13}$$

Using the final relation, along with the values of the conserved quantities $\dot M$, $\ell_{\rm in}$, $s_{\rm in}$ and $\mathcal{B}$, we can solve for the radial velocity v as a function of r in the supersonic region. This immediately gives all the other quantities.

2.3 Boundary conditions

Our model accretion flow consists of two regions: a viscous subsonic region which extends from the sonic radius $r_{\rm s}$ out to some large outer radius $r_{\rm out}$ and an inviscid supersonic region which extends from the sonic radius down to the black hole. Finding the solution in the viscous region requires solving a boundary value problem involving a number of differential equations.[2] Equations (4), (8) and (9) represent three first-order ordinary differential equations, which require three boundary conditions. In addition, the constants $\dot M$ and j are eigenvalues, which require two more boundary conditions.

[2] Once we have the solution in the viscous subsonic region, we can compute the values of $\dot M$, $\ell_{\rm in}$, $s_{\rm in}$ and $\mathcal{B}$ at $r_{\rm s}$. We can then directly calculate the solution in the supersonic region. The latter involves only algebraic equations (see Subsection 2.2), not differential equations.

Finally, the location of the sonic radius r_s has to be determined as part of the solution, so this requires yet another boundary condition. Thus, we need to supply a total of six boundary conditions.

The three differential equations (4), (8) and (9), in combination with equation (1), can be reduced to the following relation:

$$\left(\gamma c_s^2 - v^2\right)\frac{\mathrm{d}\ln|v|}{\mathrm{d}r} = \left(\Omega_K^2 - \Omega^2\right)r - \frac{2\gamma c_s^2}{r} + \frac{(\gamma-1)(\Omega r^2 - j)^2 v}{\alpha r^3 c_s}, \tag{14}$$

which becomes singular when $\gamma c_s^2 - v^2 = 0$. The radius at which this happens is the sonic radius r_s, where the flow speed $|v|$ is equal to the adiabatic sound speed $c_s\sqrt{\gamma}$. In order to have a smooth flow through r_s, the quantity on the right-hand side of equation (14) should vanish. We thus obtain the following two boundary conditions:

$$r = r_s: \quad \gamma c_s^2 - v^2 = 0, \tag{15}$$

$$r = r_s: \quad \left(\Omega_K^2 - \Omega^2\right) r_s - \frac{2\gamma c_s^2}{r_s} + \frac{(\gamma-1)\left(\Omega r_s^2 - j\right)^2 v}{\alpha r_s^3 c_s} = 0. \tag{16}$$

Viscous accretion flows have another boundary condition on the inside, which is usually applied as a no-torque condition at some radius.[3] In the most elaborate version of the theory, one would apply the no-torque condition at the black hole horizon ($r = r_g$); however, this tends to make the numerical computations very difficult. It also introduces some subtlety into the problem since the behaviour of viscosity in the supersonic plunging region of the flow is poorly understood (Narayan 1992; Kato & Inagaki 1994). In this paper, we have assumed for simplicity that viscosity vanishes inside the sonic radius. One consequence of this approximation is that the specific angular momentum of the gas Ωr^2 becomes constant in the plunging region. Motivated by this fact, we set $\mathrm{d}(\Omega r^2)/\mathrm{d}r = 0$ as a boundary condition on the viscous solution at $r = r_s$. This ensures a smooth transition across the sonic radius. Making use of equation (8), the condition can be written as

$$r = r_s: \quad \Omega r_s^2 - j = -\frac{2\alpha c_s \Omega r_s^2}{v}. \tag{17}$$

The remaining three boundary conditions are applied at the outer radius r_{out} of the solution (Yuan 1999). We choose r_{out} to be large enough that it lies well into the external uniform medium. In analogy with the Bondi problem, the temperature of the external gas, or equivalently the sound speed, and the density of the gas provide two outer boundary conditions:

$$r = r_{out}: \quad c_s = c_{out}, \tag{18}$$

$$r = r_{out}: \quad \rho = \rho_{out}. \tag{19}$$

In the numerical solutions presented here, we set $c_{out} = 10^{-3}c$, which corresponds to a temperature of 6.5×10^6 K (assuming a mean molecular weight of 0.6), a reasonable choice for the interstellar medium at the centre of a galaxy. In the case of the density, we arbitrarily select $\rho_{out} = 1$. After obtaining the solution, we can rescale the density profile by a constant factor so as to satisfy the required value of ρ_{out}. This approach is allowed by the fact that the equations are linear in the density.[4]

[3] This boundary condition is needed only for the more physical viscous stress prescription (equation 6) used here. If the shear stress is written in the simpler form αp, there is one fewer differential equation and the additional boundary condition is not needed (see Narayan et al. 1997 for a discussion). In fact, since pressure never vanishes in an accretion solution, the αp stress prescription does not have vanishing stress at any radius.

[4] This is true only because we have ignored all cooling terms. If we include a detailed cooling model, the physics will no longer be linear in ρ.

For the third boundary condition, we fix the angular velocity of the external gas:

$$r = r_{out}: \quad \Omega = \Omega_{out}. \tag{20}$$

However, we note the following complication. Because we are solving viscous accretion equations with a constant α, the solution naturally tends to a state of rigid rotation on the outside. For radii outside the Bondi radius,

$$r_B = \frac{GM}{c_{out}^2} = \frac{1}{2}\left(\frac{c}{c_{out}}\right)^2 r_g, \tag{21}$$

the black hole gravity is too weak to influence the dynamics of the gas – pressure is more important here. As a result, viscosity drives the gas towards $\mathrm{d}\Omega/\mathrm{d}r = 0$. In a real galactic nucleus, this is precisely the region where the gravitational potential of the galaxy will take over and the gas will transition to the rotation curve of the galaxy (see Quataert & Narayan 2000 for a study of Bondi accretion in such a potential). Since we have not included the galactic contribution to the potential (2), our equations enforce a rigidly rotating external medium. The problem with this is that the centrifugal acceleration $\Omega^2 r$ increases without bound at large radius, which is unphysical. To avoid this problem we choose r_{out} to be only a factor of a few (not more than 10) larger than r_B. By making this choice, we ensure that the centrifugal acceleration does not become too large on the outside. At the same time, we make sure that r_{out} is large enough for the solution to asymptote to the conditions in the external medium.

The parameter Ω_{out} determines whether the external gas is rotating slowly or rapidly. The boundary between the black hole dominated accretion flow and the external medium is located at $r \sim r_B$, and the Keplerian angular velocity $\Omega_{K,B}$ at this radius is given by

$$\Omega_{K,B} = \left(\frac{GM}{r_B^3}\right)^{1/2} = 2\left(\frac{c}{c_{out}}\right)^{-3}\frac{c}{r_g}. \tag{22}$$

We thus define the following dimensionless rotation parameter $\mathcal{R}$:

$$\mathcal{R} \equiv \frac{\Omega_{out}}{\Omega_{K,B}} = \frac{1}{2}\Omega_{out}\left(\frac{c}{c_{out}}\right)^3. \tag{23}$$

When $\mathcal{R} \ll 1$, we say that the external medium rotates slowly, whereas as $\mathcal{R}$ approaches unity, the medium rotates rapidly. We are primarily interested in the slowly rotating case.

If the external medium rotates slowly enough, the gas may be able to accrete directly into the black hole without any need for viscous transport of angular momentum. We would then have something very similar to the Bondi solution. The critical angular momentum of the external gas at which we expect this transition to take place is the specific angular momentum of the marginally stable orbit ℓ_{ms}, which for the potential (2) is

$$\ell_{ms} = \sqrt{\frac{27}{8}}\, c r_g. \tag{24}$$

Correspondingly, we can express the angular momentum of the external gas as the following dimensionless ratio:

$$\mathcal{L} \equiv \frac{\ell_{out}}{\ell_{ms}} = \frac{\Omega_{out} r_B^2}{\ell_{ms}} = 0.136\,\Omega_{out}\left(\frac{c}{c_{out}}\right)^4. \tag{25}$$

When $\mathcal{L} \gg 1$, we expect the flow to be viscously driven and to resemble an ADAF solution, whereas when $\mathcal{L} \ll 1$, the flow should be practically identical to the Bondi solution. These expectations are borne out by the numerical solutions described in Section 3. For our choice of $c_{out} = 10^{-3}c$, $\mathcal{L} = 1$ corresponds to $\mathcal{R} = 0.0037$.

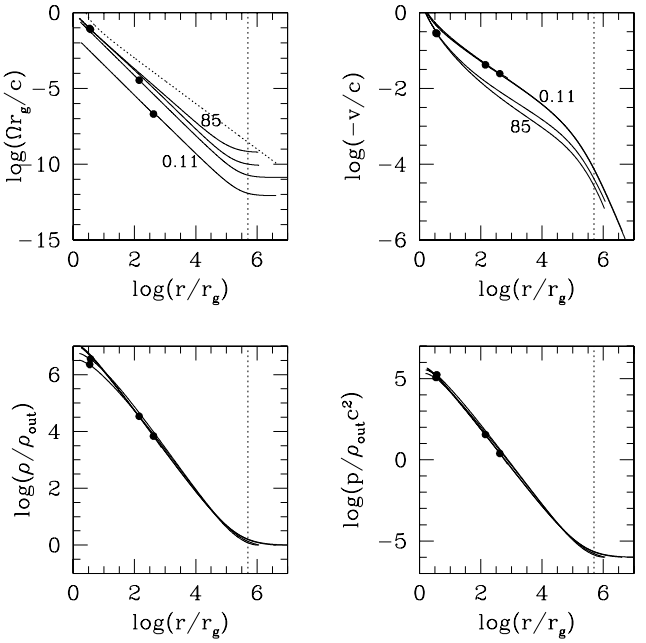

Figure 1. Representative solutions of the model equations for $\alpha = 0.1$, $\gamma = 5/3$, $c_{\rm out} = 10^{-3}c$. The four solutions shown have $(\Omega_{\rm out}, \mathcal{R}, \mathcal{L}, r_{\rm s}) = (0.624 \times 10^{-9}, 0.31, 85, 3.436), (0.851 \times 10^{-10}, 0.043, 12, 3.663), (0.132 \times 10^{-10}, 0.0066, 1.8, 142.0)$ and $(0.831 \times 10^{-12}, 0.00042, 0.11, 416.7)$, respectively. The solid dots indicate the positions of the sonic radii and are helpful for identifying the solutions. In addition, a few curves are labelled by their values of $\mathcal{L}$. The vertical dotted lines correspond to the location of the Bondi radius $r_{\rm B}$ (equation 21), and the sloping dotted line in the top left-hand panel shows the Keplerian angular frequency $\Omega_{\rm K}$.

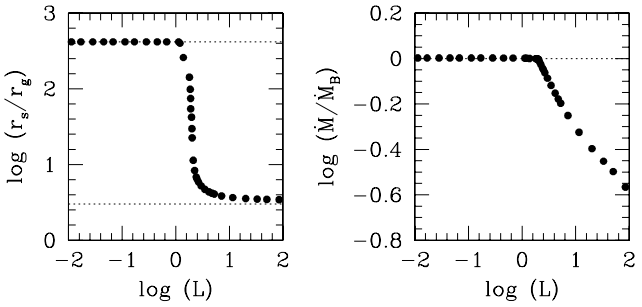

Figure 2. Left: shows the location of the sonic radius $r_{\rm s}$ as a function of the angular momentum parameter $\mathcal{L}$ for solutions with $\alpha = 0.1$, $\gamma = 5/3$, $c_{\rm out} = 10^{-3}c$. The upper dotted line indicates the sonic radius for a pure non-rotating Bondi solution, and the lower dotted line shows the radius of the marginally stable orbit $r_{\rm ms}$. Note the sudden transition from a Bondi-like flow for $\mathcal{L} < 1$ to a rotation-supported ADAF for $\mathcal{L} > 2$. Right: shows the corresponding mass accretion rates $\dot{M}$ in units of the Bondi accretion rate $\dot{M}_{\rm B}$. The mass accretion rate is only a factor of 3 smaller than the Bondi rate even when $\mathcal{L}$ is as large as $\sim 10^2$.

3 NUMERICAL RESULTS

Since the viscous accretion equations tend to be very stiff, we use a relaxation method (Press et al. 1992) to solve them.[5] Fig. 1 shows sample solutions corresponding to $\alpha = 0.1$, $\gamma = 5/3$, $c_{\rm out} = 10^{-3}c$ and $\rho_{\rm out} = 1$ (the value of $\rho_{\rm out}$ is arbitrary since we can rescale the density profile to any external density as needed, Subsection 2.3). Four solutions are shown, corresponding to $\mathcal{L} = 85$, 12, 1.8 and 0.11, respectively (compare with fig. 1 in Park 2009). Note that the rotation parameter $\mathcal{R}$ is small for all the solutions, so these truly represent slowly rotating flows. Even the most rapidly rotating solution ($\mathcal{R} = 0.31$) has a centrifugal support of only 10 per cent of Keplerian at $r = r_{\rm B}$.

The solution with $\mathcal{L} = 0.11$ – the lowest curve in the top left-hand panel of Fig. 1 – is clearly in the Bondi regime since the gas has negligible outer specific angular momentum relative to $\ell_{\rm ms}$. The sonic radius $r_{\rm s}$, shown by the black dot, is located at $417r_{\rm g}$, which is almost exactly where a pure non-rotating Bondi flow has its sonic radius for our choice of $\Phi(r)$, $c_{\rm out}$ and γ. The two solutions with $\mathcal{L} = 85$ and 12 (the highest two curves) are definitely rotation-dominated. The gas in these solutions has too much angular momentum to permit steady accretion in the absence of viscosity, so the accretion flow settles down to a viscously driven ADAF solution. Correspondingly, the sonic radius is close to the marginally stable orbit, $r_{\rm ms} = 3r_{\rm g}$. The solution with $\mathcal{L} = 1.8$ represents a transition state between the Bondi and ADAF regimes. Its sonic radius is at an intermediate location, $r_{\rm s} = 142r_{\rm g}$.

In Fig. 2, the top left-hand panel shows how the sonic radius moves as we change $\mathcal{L}$. For all values of $\mathcal{L} < 1$, $r_{\rm s}$ is located at the position one would calculate for the non-rotating Bondi problem (upper dotted line), while for $\mathcal{L}$ greater than a few, $r_{\rm s}$ is close to $r_{\rm ms}$ (lower dotted line). The transition between these two regimes is quite sudden, with most of the change happening over the range $1.5 < \mathcal{L} < 2$.

The bottom two panels in Fig. 1 show the profiles of density ρ and pressure $p = \rho c_{\rm s}^2$ for the same four solutions as in the top left-hand panel. Even though the rotation profiles of these solutions are very different, and their sonic radii move around considerably, the profiles of ρ and p are nearly identical. The insensitivity to the location of $r_{\rm s}$ is at least in part because we selected $\gamma = 5/3$, which is known to be a critical value of the adiabatic index both for the Bondi problem and for ADAFs. Nevertheless, it is clear that in many respects an ADAF is very similar to a Bondi flow.

The top right-hand panel in Fig. 1 shows the radial velocity profiles of the four solutions. We see that the radial velocity is smaller for a rotating ADAF (the solutions with $\mathcal{L} = 85$, 12) compared to a slowly rotating Bondi-like flow ($\mathcal{L} = 0.11$). Since the density profiles of both kinds of solution are nearly the same, this means that the mass accretion rates are different. This is illustrated in the right-hand panel in Fig. 2 (compare with fig. 2 in Park 2009), which shows that $\dot{M}$ decreases as the rotation of the external gas increases. The effect is quite modest, however – the total range of $\dot{M}$ in our solutions is only a factor of 3, though this is an artefact of our choice of a relatively large value of $\alpha = 0.1$.

To illustrate the effect of α, Figs 3 and 4 show results corresponding to $\mathcal{L} = 13.5$ ($\mathcal{R} = 0.05$) and six values of α: 0.316, 0.1, 0.0316, 0.01, 0.00316 and 0.001. The rotation profiles are nearly the same for different values of α, with only small variations. More interesting is the behaviour of the sonic radius, which moves in a very systematic way as α is varied. For $\alpha = 0.316$, we find $r_{\rm s} = 17.5$, which is well outside the radius of the marginally stable orbit $r_{\rm ms} = 3r_{\rm g}$. With decreasing α, $r_{\rm s}$ moves in until it is well inside $r_{\rm ms}$. The pattern is very similar to that seen in the ADAF models described in Narayan et al. (1997) and noted in many other papers (e.g. discussion of the slim disc model by Abramowicz et al. 2010).

[5] The simpler shooting method is adequate if the outer radius is not too large, e.g. $r_{\rm out}/r_{\rm g} < 10^3$. However, for realistic external media with $c_{\rm out}/c \sim 10^{-3}$, we need to calculate solutions out to $r_{\rm out}/r_{\rm g} > 10^6$. In our experience, relaxation is the only sure way to obtain such solutions.

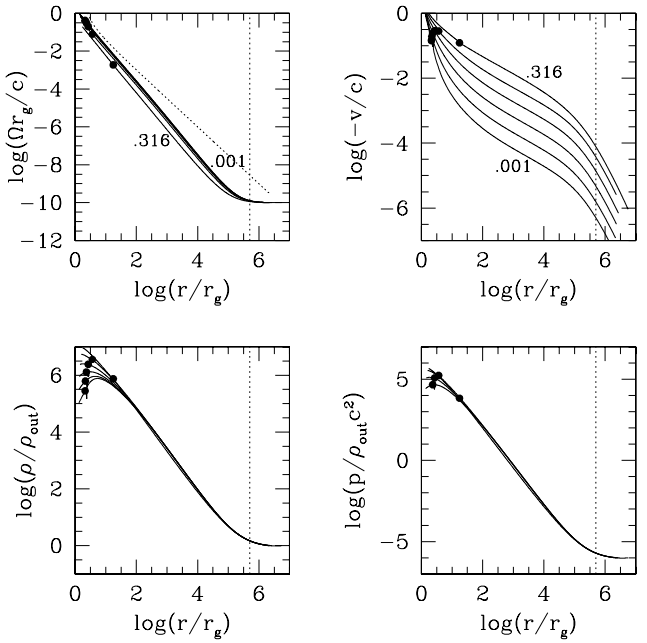

Figure 3. Solutions for $\gamma = 5/3$, $c_{\rm out} = 10^{-3}c$, $\Omega_{\rm out} = 10^{-10}$, $\mathcal{R} = 0.05$, $\mathcal{L} = 13.5$ and six values of α: 0.316, 0.1, 0.0316, 0.01, 0.00316 and 0.001. The six solutions have $r_{\rm s} = 17.54$, 3.656, 2.694, 2.335, 2.174 and 2.114, respectively. The solid dots indicate the positions of the sonic radii and are helpful for identifying the solutions. In addition, a few curves are labelled by their values of α. The vertical dotted lines correspond to the location of the Bondi radius $r_{\rm B}$, and the sloping dotted line in the top left-hand panel shows the Keplerian angular frequency $\Omega_{\rm K}$.

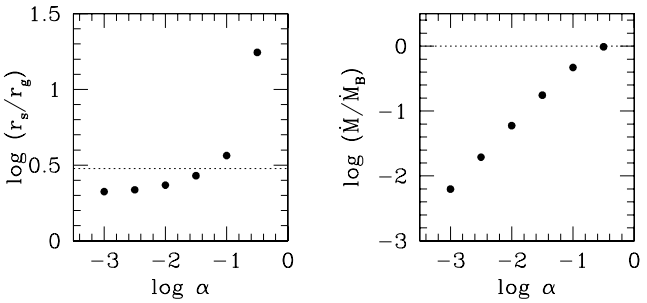

Figure 4. Left: shows the location of the sonic radius $r_{\rm s}$ as a function of the viscosity parameter α for the solutions described in Fig. 3. The dotted line indicates the radius of the marginally stable orbit $r_{\rm ms}$. Large values of α cause the sonic radius to move outside $r_{\rm ms}$, while small values of α have the opposite effect. Right: shows the corresponding mass accretion rates $\dot{M}$ in units of the Bondi accretion rate $\dot{M}_{\rm B}$. Note that $\dot{M}$ is a steep function of α, varying almost linearly. This is expected for an ADAF.

The radial velocities shown in Fig. 3 decrease proportional to α, and so do the mass accretion rates (Fig. 4, right-hand panel). This is consistent with the predictions of the analytical ADAF model described in Narayan & Yi (1994), and is in qualitative agreement with Park (2009). In particular, we agree with Park's conclusion that low angular momentum flows resemble Bondi accretion, and that their accretion rates approach the Bondi rate $\dot{M}_{\rm B}$ (which is equal to 3.65×10^8 in our units where $r_{\rm g} = c = \rho_{\rm out} = 1$) as the external rotation decreases. However, we also see some quantitative differences. Park suggests on the basis of his numerical solutions that the accretion rate scales approximately as $\dot{M}/\dot{M}_{\rm B} \sim 9\alpha/\mathcal{R}$ (our parameter $\mathcal{R}$ is the same as λ in Park's notation). We do not reproduce the scaling with $\mathcal{R}$. For instance, Fig. 2 shows that, at fixed $\alpha = 0.1$, $\dot{M}$ changes by only a factor of $\sim$3 as $\mathcal{R}$ changes by nearly a factor of 100. One reason for this difference could be that we have considered solutions with $r_{\rm B}/r_{\rm g} = 10^{5.7}$, whereas Park's solutions are closer to 10^3. A more thorough exploration of solutions in the three-dimensional space of α–$\mathcal{R}$–$(r_{\rm B}/r_{\rm g})$ would be worthwhile to map out how the accretion rate varies with these parameters.

The bottom two panels of Fig. 3 show that, with varying α, the density and pressure are largely independent of α, just as we earlier found them to be independent of $\Omega_{\rm out}$. The insensitivity of the central pressure to any parameter other than the external density $\rho_{\rm out}$ and sound speed $c_{\rm out}$ is a strong result and may have implications for jets (Section 4).

4 DISCUSSION

The primary goal of this paper was to estimate the rate at which mass accretes on to a supermassive black hole from rotating gas in the nucleus of a galaxy. We find that the answer depends on both the dimensionless rotation parameter of the gas $\mathcal{R}$ (equation 23) and the viscosity parameter α (equation 5). For fixed $\alpha = 0.1$, the accretion rate is within a factor of a few of the Bondi rate for all values of $\mathcal{R}$ (Fig. 2), i.e. for this value of α accretion is nearly as efficient in the presence of rotation as in its absence (the classic Bondi problem). Fig. 4 shows the variation of $\dot{M}$ for fixed $\mathcal{R} = 0.05$ (a reasonable value; see Inogamov & Sunyaev 2010) and different values of α. Here the variation is much larger. The accretion rate is suppressed by a large factor when $\alpha \ll 1$. Hence, the answer to our primary question depends very much on the value of α.

King, Pringle & Livio (2007) have examined a variety of observational evidence and conclude that many observed accretion discs have $\alpha \sim 0.1$–0.4. In addition, Sharma et al. (2006) argue that ADAFs have, if at all, even larger values of α compared to standard thin discs. Thus, the models with $\alpha = 0.316$ and 0.1 in Fig. 4 may be the best match to real radiatively inefficient accretion flows in galactic nuclei. If so, we can expect viscous accretion via an ADAF to be quite efficient in galactic nuclei: $\dot{M}_{\rm ADAF} \sim (0.3 - 1) \times \dot{M}_{\rm B}$.

As discussed in Section 1, our picture is that a fraction $\eta_{\rm acc}$ of the accretion energy near the black hole is somehow converted to jet mechanical energy. If the accretion rate is equal to the Bondi rate, then observations require about 2 per cent of $\dot{M}_{\rm B}c^2$ to be transferred to the jet. From the estimates given above, we see that accretion of rotating gas via an ADAF requires an efficiency of perhaps $\eta_{\rm acc} \sim$ 5 per cent. While we do not have a model of how the jet is actually launched, an efficiency of 5 per cent does not appear implausible.

It should be emphasized that the present study differs from most previous discussions of this problem in the literature in that we consider a steady viscous flow extending from beyond the Bondi radius down to the black hole horizon. Viscosity enables our solutions to overcome the centrifugal barrier and to accrete steadily, just as in the standard thin accretion disc model (Shakura & Sunyaev 1973; Frank, King & Raine 2002). In contrast, most other studies of quasi-spherical accretion with rotation (except Park 2009, see Section 1) have considered inviscid accretion. Those results depend critically on the assumption that accretion is arrested once the gas hits the centrifugal barrier.

From our numerical solutions, we can calculate the time required for gas to travel from the Bondi radius down to the black hole. For the two models with $\alpha = 0.316$ and 0.1 in Fig. 4, the accretion time $t_{\rm ADAF}$ for the ADAF solution is no more than twice as long as the accretion time $t_{\rm B}$ in the non-rotating Bondi solution. Even for the

rapidly rotating solution with $\mathcal{R} = 0.31$ in Fig. 2, $t_{\rm ADAF}$ is only $\sim 3t_{\rm B}$.[6] This is very encouraging. For a turbulent external medium, we expect the rotation of the external gas near the Bondi radius to vary on a time-scale of the order of tens of $t_{\rm B}$ (assuming a turbulent Mach number $\sim$0.1; Inogamov & Sunyaev 2010). Since our ADAF solutions have an accretion time much shorter than the turbulence time, there is no problem setting up the steady-state conditions we assume. More importantly, the short accretion time guarantees that any feedback from the ADAF via jets will occur rapidly compared to the dynamical time of the external medium. Such instantaneous feedback is generally assumed in most current models of feedback.

While we have focused so far on the accretion flow as the source of jet power, a popular alternative hypothesis involves the black hole. Blandford & Znajek (1977) developed a scenario in which the rotational energy of a spinning black hole is tapped by a magnetic field and carried away in a magnetized jet. For a magnetic flux Φ_B threading the horizon, Tchekhovskoy, Narayan & McKinney (2010) give a fairly accurate estimate of the jet power in geometrized units ($GM = c = 1$):

$$P_{\rm j} = k\Phi_B^2\Omega_{\rm H}^2, \quad \Omega_{\rm H} = \frac{a_*}{2r_{\rm H}}, \quad r_{\rm H} = 2M\left[1 + (1-a_*)^2\right]^{1/2}, \quad (26)$$

where $k \approx 0.05$ is a dimensionless number that depends weakly on the field geometry, $a_* \equiv a/M$ is the dimensionless spin parameter of the black hole, and $r_{\rm H}$ and $\Omega_{\rm H}$ are the radius and angular frequency of the black hole horizon. The magnetic flux is given by $\Phi_B = 4\pi r_{\rm H}^2 |B|_{\rm H}$, where $|B|_{\rm H}$ is the field strength at the horizon. Thus,

$$P_{\rm j} = 32\pi^3 k p_{\rm mag} r_{\rm H}^2 a_*^2 \approx 50 p_{\rm mag} r_{\rm H}^2 a_*^2, \quad (27)$$

where $p_{\rm mag} = |B|_{\rm H}^2/8\pi$ is the magnetic pressure at the horizon.

To maintain a magnetic field on the horizon, it is necessary to keep the field lines in place by means of an external pressure. We assume that this pressure is supplied by the accretion flow. Consider first the Bondi non-rotating solution. In our units ($r_{\rm g} = c = \rho_{\rm out} = 1$), the thermal pressure of the Bondi solution at $r = 2r_{\rm g}$ is[7] $p_{\rm therm}(2r_{\rm g}) = 3.34 \times 10^5$, and the ram pressure is $p_{\rm ram}(2r_{\rm g}) = \rho v^2 = 6.51 \times 10^6$, giving a total pressure of $p_{\rm tot}(2r_{\rm g}) = 6.85 \times 10^6$. We assume that the total pressure is what confines the central field and write the magnetic pressure at the base of the jet as $P_B = \eta_B p_{\rm tot}(2r_{\rm g})$, where $\eta_B < 1$ is a proportionality constant. We also replace $r_{\rm H}$ by $r_{\rm g}$ in equation (27), which is an overestimate for a rapidly spinning hole but is probably a reasonable simplification. We then find

$$\text{Bondi}: \qquad P_{\rm j} \approx 3.4 \times 10^8 \eta_B a_*^2 \approx \eta_B a_*^2 \dot{M}_{\rm B} c^2. \quad (28)$$

This interesting result shows that the jet power scales directly with the Bondi accretion energy rate $\dot{M}_{\rm B}c^2$ and varies strongly with the spin of the black hole. Our guess is that η_B is probably in the range 0.1–1. Therefore, provided the black hole does not rotate too slowly, a Bondi flow could easily support the jets seen in observations.

We now compute the central pressures in the ADAF solutions. The four solutions shown in Fig. 2 have pressures ranging from $p_{\rm tot}(2r_{\rm g}) = 1.49 \times 10^6$ for $\mathcal{R} = 0.31$ to $p_{\rm tot}(2r_{\rm g}) = 6.84 \times 10^6$ for $\mathcal{R} = 0.00046$, while the $\alpha = 0.316$ and 0.1 solutions in Fig. 4 have $p_{\rm tot}(2r_{\rm g}) = 6.27 \times 10^6$ and 2.59×10^6, respectively. These are the solutions most relevant for our problem, and their pressures are between 20 and 100 per cent of the Bondi pressure. Thus, we obtain the following estimate for the jet power in the presence of an ADAF:

$$\text{ADAF}: \qquad P_{\rm j} \approx (0.2-1) \times \eta_B a_*^2 \dot{M}_{\rm B} c^2. \quad (29)$$

The jet efficiency factor in this model is $\eta_{\rm j} = (0.2-1) \times \eta_B$ and a net efficiency of 2 per cent seems quite plausible.

To summarize, in terms of energetics at least, we have two viable mechanisms to power jets via accretion in galactic nuclei: (i) by tapping a fraction of the accretion energy and (ii) by confining a strong magnetic field around a spinning black hole and extracting energy from the hole. Neither mechanism requires us to postulate extreme conditions or to stretch parameters. However, all of our results are based on the simple one-dimensional model described in Section 2. Unfortunately, there are several important caveats that need to be discussed.

Narayan & Yi (1994, 1995a) showed that the accreting gas in an ADAF has a positive Bernoulli parameter $\mathcal{B}$ (see equation 13 for the definition). This means that the gas is gravitationally unbound, and so these authors suggested that ADAFs would have strong outflows and jets. The mass conservation equation (1) explicitly ignores such outflows. How strong the outflows are is difficult to estimate from first principles, though Blandford & Begelman (1999) suggested that the effect may be so strong that $\dot{M}_{\rm ADAF}$ at the black hole might be reduced by orders of magnitude.

Numerical hydrodynamic simulations have confirmed that the mass accretion rate is indeed suppressed (Igumenshchev & Abramowicz 1999, 2000; Stone, Pringle & Begelman 1999; Igumenshchev 2000), though there is no consensus on whether gas truly escapes to infinity, or if the Bernoulli parameter is even relevant (Abramowicz, Lasota & Igumenshchev 2000). If outflows are as strong as Blandford & Begelman (1999) suggest, both jet mechanisms we have discussed here are impossible. One mechanism depends directly on $\dot{M}_{\rm ADAF}$, while the other depends on the central pressure $p_{\rm tot}$ which is roughly proportional to $\dot{M}_{\rm ADAF}$. If there are heavy outflows, there is just not enough energy to power the observed jets.

Fig. 5 shows the variation of $\mathcal{B}$ with r for the solutions shown in Figs 1 and 3. We have normalized $\mathcal{B}$ by the local gravitational potential $|\Phi(r)|$ to obtain a dimensionless measure of how unbound the gas is at each radius. All the solutions start with a large value of $\mathcal{B}/|\Phi|$ outside the Bondi radius, but this just means that the gas out there has a finite thermal energy but very little gravitational binding energy. As the gas flows in, $\mathcal{B}$ hardly changes, while Φ increases rapidly in magnitude, so the ratio $\mathcal{B}/|\Phi|$ decreases rapidly.

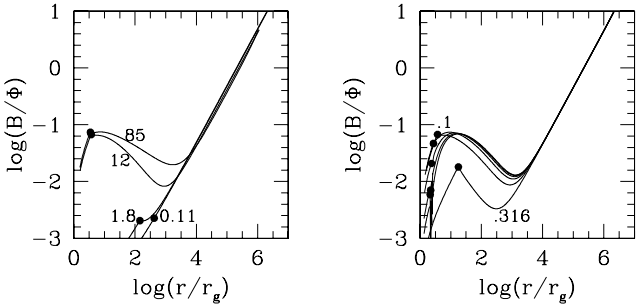

Figure 5. Variation with radius of the Bernoulli parameter $\mathcal{B}$ (equation 13), normalized by the gravitational potential, for the four solutions shown in Fig. 1 (left-hand panel) and the six solutions shown in Fig. 3 (right-hand panel). The solid dots indicate the positions of the sonic radii. Curves are labelled by their values of $\mathcal{L}$ in the left-hand panel and α in the right-hand panel.

[6] For very small values of α, we do we find $t_{\rm ADAF} \gg t_{\rm B}$, e.g. for $\alpha = 0.001$, $\mathcal{R} = 0.05$, we obtain $t_{\rm ADAF}/t_{\rm B} = 156$. However, such low values of α seem unlikely.

[7] We cannot use $r = r_{\rm g}$ because our Newtonian potential (2) is singular there.

In the case of the Bondi-like solution with $\mathcal{L} = 0.11$, the decrease continues all the way down to the horizon and there is no tendency to form an outflow. The ADAF solutions, on the other hand, follow the Bondi solution down to $r \sim 10^3 r_g$, after which viscous dissipation causes $\mathcal{B}/|\Phi|$ to increase up to a maximum value of about 0.1. We do not know if this value is large enough to strongly suppress the mass accretion rate on to the black hole. However, since the Bernoulli parameter is large only over a limited range of radius, it is conceivable that outflows reduce the mass accretion rate in the ADAF solutions by no more than a factor of a few, rather than by orders of magnitude. In this case, both of our jet mechanisms are likely to survive.

Our model assumes a single point source of gravitation, whereas a realistic galactic nucleus has significant stellar mass from the inner galaxy and any nuclear star cluster. This will make the outer gas more gravitationally bound than appears from Fig. 5. Radiative cooling (which is ignored in our model) can also have an effect. Using the gas properties at the Bondi radius given in Allen et al. (2006) for M87 we find that the radiative cooling time is about 2.5 per cent of the flow time (r/c_s). The ratio of these time-scales increases at smaller radii, making radiative cooling unimportant there. Compton cooling, however, increases with decreasing radius and may be important at precisely those inner radii where $\mathcal{B}$ shows an increase in Fig. 5. Thus, the importance of the Bernoulli parameter may be reduced even further.

Another important effect pointed out by Narayan & Yi (1994) is that viscous dissipation, coupled with the lack of radiative cooling, causes the entropy of the gas in an ADAF to increase inwards, making the flow convectively unstable by the Schwarzschild criterion. Convective effects have not been included in the one-dimensional model we have considered in this paper. Narayan, Igumenshchev & Abramowicz (2000) and Quataert & Gruzinov (2000) discussed the physics of convection-dominated accretion flows (CDAFs) and concluded that such flows would differ enormously from ADAFs. In particular, if one considers a self-similar model, the density, pressure and mass accretion rate of a CDAF, as measured at the black hole, are predicted to be a factor of $\sim r_g/r_B \sim 10^{-5}$ (for our models) times the corresponding values for an ADAF with the same outer boundary conditions. Even if the real effect is only a small fraction of this analytical prediction, it would reduce jet power to a level far below that observed.

Numerical hydrodynamic simulations confirm the presence of convection in ADAFs (Igumenshchev & Abramowicz 1999, 2000; Stone et al. 1999; Igumenshchev, Abramowicz & Narayan 2000) and indicate substantial suppression of the mass accretion rate into the black hole. This is problematic for jet production. However, the relative importance of ADAFs versus CDAFs has been debated (e.g. Igumenshchev & Abramowicz 1999; Abramowicz et al. 2002; Lu, Li & Gu 2004), and the issue is still unresolved.

A measure of convective instability is the Brunt–Vaisala frequency N which for a spherically symmetric system is given by

$$N^2 = -\frac{1}{\rho}\frac{\mathrm{d}p}{\mathrm{d}r}\frac{\mathrm{d}\ln(p^{1/\gamma}/\rho)}{\mathrm{d}r}. \quad (30)$$

A system is convectively unstable if $N^2 < 0$. When this happens, the quantity $|N| \equiv \sqrt{-N^2}$ measures the growth rate of the instability. We imagine that convection is important and takes over the dynamics of the flow only when the growth time-scale of the instability is shorter than the accretion time $t_{acc} \equiv r/|v|$, whereas in the opposite limit, we expect convection to be a minor perturbation. Motivated by this argument, we show in Fig. 6 the profiles of the dimensionless quantity $-N^2 t_{acc}^2$ versus r for a selection of our numerical solutions.

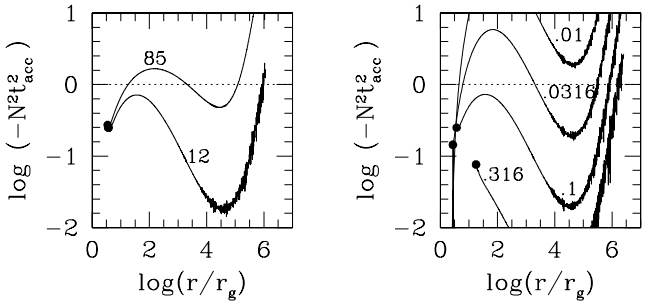

Figure 6. Left: variation with radius of the quantity $-N^2 t_{acc}^2$, which is a measure of convective instability, for two of the four solutions shown in Fig. 1. (The other two are below the bottom of the plot.) The dotted line indicates our nominal threshold for becoming convection-dominated. The more rapidly spinning solution ($\mathcal{L} = 85$) goes above the dotted line over a range of radius, and we expect it to become a CDAF in this zone. The less rapidly rotating solution ($\mathcal{L} = 12$) lies below the dotted line and probably will not become a CDAF. Right: corresponding results for the solutions shown in Fig. 3. The two solutions with $\alpha = 0.316$ and 0.1 lie below the dotted line and will not be convection-dominated, while the solutions with smaller values of α are expected to become CDAFs. Note that none of the curves in the two panels extends inside the sonic radius. This is because we have assumed the flow to be inviscid once it becomes supersonic. The specific entropy is then constant (Subsection 2.2) and $N^2 = 0$.

Most of the solutions of interest to us, viz. those with relatively large values of α and small rotation parameters $\mathcal{R}$, have $-N^2 t_{acc}^2 < 1$. Convection is probably unimportant in these cases. The results shown in the right-hand panel agree with the α trend discussed by Igumenshchev & Abramowicz (1999) and Lu et al. (2004).

In the discussion so far, we have ignored the effect of magnetic fields. Magnetohydrodynamic (MHD) simulations of ADAFs (Hawley, Balbus & Stone 2001; Stone & Pringle 2001; Igumenshchev & Narayan 2002; Igumenshchev, Narayan & Abramowicz 2003; Pen, Matzner & Wong 2003; Igumenshchev 2006, 2008; Pang et al. 2010) have not so far exhibited strong unbound winds, but they nevertheless have shallow density profiles and reduced $\dot{M}$. The flows exhibit vigorous turbulence and they transport energy outwards, just as one expects with a convective flow. However, whether or not the turbulence can be described as convection is unclear (Balbus & Hawley 2002; Narayan et al. 2002; Pen et al. 2003).

From the point of view of our present study, the relevant question is how much is the mass accretion rate suppressed relative to the Bondi rate as a result of MHD effects. The best scalings from current simulations suggest that the accretion rate, and therefore the jet power, is reduced by at least three orders of magnitude. Moreover, $\dot{M}$ is found to be reduced substantially even in the case of a non-rotating Bondi flow (Igumenshchev & Narayan 2002; Igumenshchev 2006). This last result is particularly worrisome in view of the results shown in Fig. 6. There it appeared that, so long as α is relatively large and the rotation is small, hydrodynamic convection and the consequent suppression of $\dot{M}$ are not an issue. However, it appears that magnetic fields completely alter the situation and strongly suppress even Bondi accretion. This effect needs to be confirmed with further studies and the physics of the phenomenon needs to be identified.

Apart from convection, thermal conduction might also modify the dynamics of radiatively inefficient accretion (e.g. Johnson & Quataert 2007; Sharma, Quataert & Stone 2008; Shcherbakov & Baganoff 2010). Numerical MHD simulations including conduction and covering an adequate range of radius are yet to be carried out.

If any of the effects discussed here succeeds in strongly suppressing the mass accretion rate in quasi-spherical accretion flows, we would be left with the puzzle of why the observed jet power P_j in many nearby low-luminosity galactic nuclei tracks the estimated Bondi mass accretion rate $\dot{M}_B$ (Section 1): $\eta_j \equiv P_j/\dot{M}_B c^2 \sim 2$ per cent. The observed jets would require a different explanation that is not related to a hot accretion flow, and the apparent correlation with properties of hot gas at the Bondi radius must be a coincidence.

A disc of dense cool gas emitting optical lines is often seen in the nuclei of elliptical galaxies. Macchetto et al. (1997) have studied the gas distribution in M87 and used the kinematics of the gas to estimate the mass of the black hole. The result is slightly less than that now determined from stellar kinematics by Gebhardt & Thomas (2009). The gas disc has a central hole a few pc in size. Linewidths are large, possibly indicating the action of non-gravitational forces in this and other elliptical galaxies (Verdoes-Kleijn, van der Marel & Noel-Storr 2006). We do not think that small masses of such cool gas are incompatible with the existence of a giant ADAF.

Finally, we note that estimates showing that Bondi accretion cannot yield a sufficient mass accretion rate (e.g. Rafferty et al. 2006) are based on the temperature and density values inferred at radii far outside r_B. Small quantities of cooler gas at the centre, say at 0.7 keV instead of 3 keV, which is in pressure equilibrium with the surrounding gas would have a correspondingly higher density and allow a much higher Bondi flow rate ($\dot{M}_B \propto T^{-5/2}$). Such cool gas is often observed in nearby clusters where the innermost regions are spatially resolved. The rate will in practice be even higher than this simple scaling as the pressure will be higher at the Bondi radius due to the weight of intervening gas.

5 SUMMARY

We have shown in this paper that accretion can occur from a hot atmosphere at close to the Bondi rate, provided the external gas near the Bondi radius rotates relatively slowly (less than a few tens of per cent of the Keplerian rate) and the viscosity parameter α is fairly large ($\geq$0.1). The non-radiative numerical ADAF solutions computed here may be relevant to the nuclei of massive elliptical galaxies hosting a central black hole surrounded by a hot gaseous atmosphere. The mass accretion rate is large enough that it requires only a small fraction ($\sim$2–5 per cent) of the accretion energy to power the observed jets in nearby elliptical galaxies. At the same time, the jets can heat the surrounding gas and prevent the hot atmosphere from radiatively cooling and collapsing into the centre. This feedback mechanism could also have an effect on the evolution of the galaxy itself. These results require that mass outflows (other than that associated with the jets), convective energy transport and MHD effects are weaker than usually assumed.

ACKNOWLEDGMENTS

We thank the referee for a thoughtful review. RN thanks the Institute of Astronomy, Cambridge, for hospitality while much of this work was carried out. RN's research was supported in part by NSF grant AST-1041590 and NASA grant NNX11AE16G. ACF thanks the Royal Society for support.

REFERENCES

Abramowicz M. A., Chen X., Kato S., Lasota J.-P., Regev O., 1995, ApJ, 438, L37
Abramowicz M. A., Lasota J.-P., Igumenshchev I. V., 2000, MNRAS, 314, 775
Abramowicz M. A., Igumenshchev I. V., Quataert E., Narayan R., 2002, ApJ, 565, 1101
Abramowicz M. A., Jaroszyński M., Kato S., Lasota J.-P., Różańska A., Sadowksi A., 2010, A&A, 521, 15
Allen S. W., Dunn R. J. H., Fabian A. C., Taylor G. B., Reynolds C. S., 2006, MNRAS, 372, 21
Balbus S. A., Hawley J. F., 2002, ApJ, 573, 749
Blandford R. D., Begelman M. C., 1999, MNRAS, 303, L1
Blandford R. D., Znajek R. L., 1977, MNRAS, 179, 433
Bondi H., 1952, MNRAS, 112, 195
Chen X., Abramowicz M. A., Lasota J. P., 1997, ApJ, 476, 61
Croton D. J., Springel V., White S. D. M., De Lucia G., Frenk C. S. et al., 2006, MNRAS, 365, 11
Cuadra J., Nayakshin S., Springel V., di Matteo T., 2006, MNRAS, 366, 358
Di Matteo T., Allen S. W., Fabian A. C., Wilson A. S., Young A. J., 2003, ApJ, 582, 133
Fabian A. C., Rees M. J., 1995, MNRAS, 277, L55
Frank J., King A., Raine D., 2002, Accretion Power in Astrophysics. Cambridge Univ. Press, Cambridge
Gebhardt K., Thomas J., 2009, ApJ, 700, 1690
Hawley J. F., Balbus S. A., Stone J. M., 2001, ApJ, 554, L49
Hlavecek-Larrondo J., Fabian A. C., 2011, MNRAS, 413, 313
Hopkins P. F., Hernquist L., Cox T. J., di Matteo T., Robertson B., Springel V., 2006, ApJS, 163, 1
Igumenshchev I. V., 2000, MNRAS, 314, 54
Igumenshchev I. V., 2006, ApJ, 649, 361
Igumenshchev I. V., 2008, ApJ, 677, 317
Igumenshchev I. V., Abramowicz M. A., 1999, MNRAS, 303, 309
Igumenshchev I. V., Abramowicz M. A., 2000, ApJS, 130, 463
Igumenshchev I. V., Narayan R., 2002, ApJ, 566, 137
Igumenshchev I. V., Abramowicz M. A., Narayan R., 2000, ApJ, 537, L27
Igumenshchev I. V., Narayan R., Abramowicz M. A., 2003, ApJ, 592, 1042
Inogamov N. A., Sunyaev R. A., 2010, Astron. Lett., 36, 835
Johnson B. M., Quataert E., 2007, ApJ, 660, 1273
Kato S., Inagaki S., 1994, PASJ, 46, 289
Kato S., Fukue J., Mineshige S., 2008, Black-Hole Accretion Disks – Towards a New Paradigm, Kyoto Univ. Press, Kyoto, Japan
King A. R., Pringle J. E., Livio M., 2007, MNRAS, 376, 1740
Kley W., Papaloizou J. C. B., 1997, MNRAS, 285, 239
Krumholz M. R., McKee C. F., Klein R. I., 2005, ApJ, 618, 757
Lu J.-F., Li S.-N., Gu W.-M., 2004, MNRAS, 352, 147
Macchetto F., Marconi A., Axon D., Capetti A., Sparks W., Crane P., 1997, ApJ, 489, 579
McNamara B. R., Nulsen P. E. J., 2007, ARA&A, 45, 117
Manmoto T., Kato S., Nakamura K. E., Narayan R., 2000, ApJ, 529, 127
Narayan R., 1992, ApJ, 394, 261
Narayan R., McClintock J. E., 2008, New Astron. Rev., 51, 733
Narayan R., Yi I., 1994, ApJ, 428, L13
Narayan R., Yi I., 1995a, ApJ, 444, 231
Narayan R., Yi I., 1995b, ApJ, 452, 710
Narayan R., Kato S., Honma F., 1997, ApJ, 476, 49
Narayan R., Mahadevan R., Quataert E., 1998, in Abramowicz M. A., Bjornsson G., Pringle J. E., eds, Theory of Black Hole Accretion Disks. Cambridge Univ. Press, Cambridge, p. 148
Narayan R., Igumenshchev I. V., Abramowicz M. A., 2000, ApJ, 539, 798
Narayan R., Quataert E., Igumenshchev I. V., Abramowicz M. A., 2002, ApJ, 577, 295
Paczyński B., Wiita P. J., 1980, A&A, 88, 23
Pang B., Pen U.-L., Matzner C. D., Green S. R., Liebendörfer M., 2010, preprint (arXiv:1011.5498)
Park M. G., 2009, ApJ, 706, 637
Pen U.-L., Matzner C. D., Wong S., 2003, ApJ, 596, L207
Pizzolato F., Soker N., 2005, ApJ, 632, 821
Popham R., Gammie C. F., 1998, ApJ, 504, 419

Press W. H., Teukolsky S. A., Vetterling W. T., Flannery B. P., 1992, Numerical Recipes in FORTRAN. The Art of Scientific Computing. Cambridge Univ. Press, Cambridge
Proga D., Begelman M. C., 2003, ApJ, 582, 69
Quataert E., Gruzinov A., 2000, ApJ, 539, 809
Quataert E., Narayan R., 2000, ApJ, 528, 236
Rafferty D., McNamara B. R., Nulsen P. E. J., Wise M. W., 2006, ApJ, 652, 216
Shakura N. I., Sunyaev R. A., 1973, A&A, 24, 337
Sharma P., Hammett G. W., Quataert E., Stone J. M., 2006, ApJ, 637, 952
Sharma P., Quataert E., Stone J. M., 2008, MNRAS, 389, 1815
Shcherbakov R. V., Baganoff F. K., 2010, ApJ, 716, 504
Stone J. M., Pringle J. E., 2001, MNRAS, 322, 461
Stone J. M., Pringle J. E., Begelman M. C., 1999, MNRAS, 310, 1002
Tchekhovskoy A., Narayan R., McKinney J. C., 2010, ApJ, 711, 50
Verdoes-Kleijn G., van der Marel R. P., Noel-Storr J., 2006, AJ, 131, 1961
Yuan F., 1999, ApJ, 521, L55

This paper has been typeset from a TEX/LATEX file prepared by the author.